RSC Advances

ROYAL SOCIETY OF CHEMISTRY

www.rsc.org/advances

Journal Name

ARTICLE

Mechanism of Pd-catalyzed C(sp^3)–H Activation of Aliphatic Amines: An Insight from DFT Calculations

Received 00th January 20xx,
Accepted 00th January 20xx

DOI: 10.1039/x0xx00000x

www.rsc.org/

Ye Zhang, Zheng-Hang Qi, Gui-Yu Ruan, Yi Zhang, Wei Liu,* and Yong Wang*

A theoretical understanding of the Pd-catalyzed C(sp^3)–H activation of aliphatic amines has been examined using the B3LYP density functional theory. The concerted metalation–deprotonation (CMD) mechanism is identified in the rate-determining steps of all possible reaction pathways. The rate- and regio-determining step of the catalytic cycle is deprotonation of C_{methyl}–H bond through a six-membered cyclopalladation transition state. According to the relative activation barriers, the C_{methyl}–H activation is kinetically and thermodynamically more favorable than the C_{ethyl}–H activation. More important, the only acetoxylation product is located, ignoring the diethyl-substituted or the dimethyl-substituted in the morpholine and not producing the lactone amines molecules, which is in good agreement with the experimental observations.

Introduction

Transition-metal–catalyzed C–H bond functionalizations have attracted increasing interests in organic synthesis to transform unreactive C–H bonds into carbon–carbon or carbon-heteroatom bonds.[1] Over the years, transition metals coordinate to a substrate could promote the cleavage of the C–H bond, which is reactive toward a series of reactions.[2] More recently, palladium-catalyzed tandem C–H activation and C–C coupling reactions have emerged,[3,4] which are available for improving synthetic efficiency and economically as a powerful and popular strategy. In the past several decades, lots of studies have been reported on the Pd^0/Pd^{II} intermediates.[5] Similarly, the high Pd^{III} and Pd^{IV} complexes as activate intermediates have also been widely proposed.[6] Ritter, Derat, Canty, and co-workers have carried out extensive studies to investigate the binuclear Pd intermediates, which are proved to be important in the palladium-catalyzed C–H functionalizations. They found the process from lower-valent Pd^I/Pd^{II} to the high-valent Pd^{III} or Pd^{IV} prefers to take place through pentacoordinated complexes rather than octahedric ones.[7,8] In particular, the $Pd(OAc)_2$-catalyst systems have been successfully employed for the C–H activation of a wide range of substrates.[9] In contrast to the wealth of methods recently developed for the functionalization of arenes and heteroarenes C(sp^2)–H bonds,[10] the functionalization of aliphatic C(sp^3)–H bonds[11] remains a challenging task. Especially, the regioselectivity of the C–H activation reactions particularly presents a more complicated problem.[12] Fortunately, the presence of directing groups were found effectively to control selectivity for C–H activation of a complex substrate containing multiple C–H bonds. For example, the reported C(sp^3)–H activations with directed groups, such as the monodendate substituted pyridines (Eq1),[13] and the bidentate 8-Aminoquinoline (Eq2),[14] could achieve through a five-membered metallacycle intermediate, respectively.[2a,11c,15] Notably, a comprehensive mechanism of the C–H bond cleavage step by the concerted metalation–deprotonation (CMD) pathway has been demonstrated to be important in further development of cross-coupling reactions using transition-metal catalysts.[16]

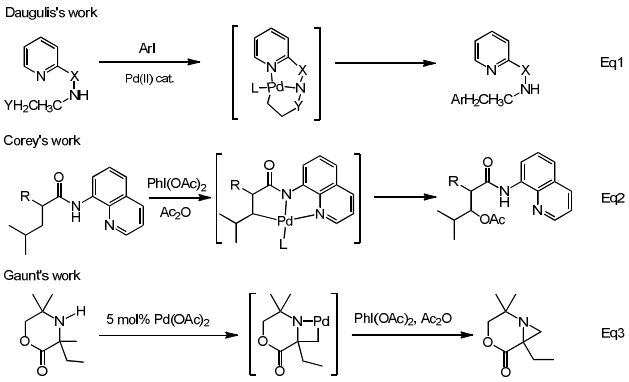

Scheme 1 Some reported site-selective palladium-catalyzed C–H activations.

While many studies described above have focused on palladium catalyzed C(sp^3)–H activation of aryl halides via 5-

College of Chemistry, Chemical Engineering and Materials Science, Soochow University, Suzhou 215123, P. R. China. E-mail: yowang@suda.edu.cn; weiliu@suda.edu.cn

Electronic supplementary information (ESI) available Cartesian coordinates for all optimized reactants, intermediates, transition states, and products reported in this work. See DOI: 10.1039/x0xx00000x

membered palladacycle intermediates. In contrast, in 2014, the Gaunt's group studied the palladium-catalyzed C(sp^3)–H activation of aliphatic amines through a four-membered cyclopalladation intermediate, which described the selective transformation of a methyl group with unprotected secondary amine,[17] as depicted in Scheme 1 (Eq3). In this context, theoretical mechanistic investigations are of vital importance. As one part of our ongoing work toward understanding the mechanisms of Pd-catalyzed C–H activation, we are interested in examining the mechanisms of regiospecific dehydrogenative cross-coupling of aliphatic amines as shown in Scheme 1, using $PhI(OAc)_2$ as the terminal oxidant.

Herein, the plausible mechanism on $Pd(OAc)_2$-catalyzed C(sp^3)–H activation of aliphatic amines (**A**) was shown in Scheme 2. Firstly, the palladium coordinate with the substrate to generate the activated precursor intermediate (**B**), acetate act as an internal base to cleave the C–H bond via a six-membered transition state (**C**) by a concerned metalation-deprotonation (CMD) pathway, subsequently leading to a four-membered cyclopalladation intermediate (**D**). Next, a Pd(IV) intermediate (**E**) was located by a Pd(II) precursor and oxidative $PhI(OAc)_2$. Finally, reductive elimination from penta-coordinated Pd(IV) complex **E** may take place via the C–N cyclization transition state (**F**) to form the aziridene product (**G**) and to help regenerate the Pd-catalyst back to its native oxidation state during the reaction cycle.

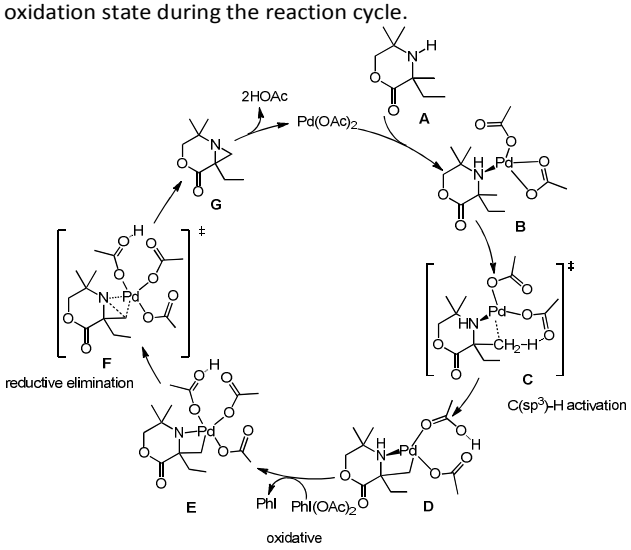

Scheme 2 The proposed mechanism of the catalytic cycle.

Computational details

All calculations in this work were performed by the density functional theory with the three-parameter hybrid functional (B3LYP)[18] using Gaussian09 program package (G09),[19] employing the true effective core potentials (ECP) such as LANL2DZ[20] basis/pseudopotential for Pd, and 6-31G(d,p)[21] for all other nonmetal atoms. Frequency calculations were performed on all gas-phase optimized geometries to verify stationary points as minima (no imaginary frequencies) or transition states (only one imaginary frequency). Intrinsic reaction coordinate (IRC)[22] analysis was carefully carried out to confirm whether it connected the correct configurations of reactant and product on the potential energy surface. All the energies discussed in the main text are relative solvation-free energies (ΔG_{sol}), adding the solvation corrections to the computed gas phase relative free energies (ΔG_{298}). According to the experiments, toluene was used as the solvent with the SMD[23] model. Optimized structures were visualized by the CYLview program.[24]

Results and discussions

Methyl-C–H activation *vs* Ethyl-C–H activation. As shown in Figure 1, two possible C–H activation pathways were discussed, including C_{methyl}–H activation and C_{ethyl}–H activation. Firstly, amine coordinates to $Pd(OAc)_2$ to form **INT-1,** which is more stable than the starting reactants by 13.1 kcal/mol. In current paper, the *S*-configurations of C–H activation were mainly discussed with similar mechanism as R isomers. Starting from **INT-1**, two possible CMD C_{methyl}–H activation and C_{ethyl}–H activation may take place. During C_{methyl}–H activation, the rate-determining six-membered transition state **TS-1** connects intermediate **INT-1** and **INT-2** with a barrier of 27.2 kcal/mol. In **TS-1**, one H atom of methyl group would be abstracted by one AcO^- as the acetate ligand-assisted C–H activation mechanism.[11c,25]As shown in Figure 1, it should be noted that a four-membered metallacycle intermediate **INT-2** is formed. In contrast, the *S*-configuration C_{ethyl}–H activation takes place through a six-membered transition **TS-1-a** with a relatively higher barrier of 35.4 kcal/mol than that of C_{methyl}–H activation, suggesting a favorable C_{methyl}–H activation, which is in agreement with the experimental results.[13] Also interestingly, after **TS-1-a**, a five-membered palladacycle intermediate **INT-2-a** is located by 1.8 kcal/mol less stable than **INT-2**. As shown in Figure 1, it should be noted that a four-membered metallacycle intermediate **INT-2** is formed, which is energetically lower than the former intermediate **INT-1** by 4 kcal/mol. After **INT-2**, a more stable Pd(IV) intermediate **INT-3** is located by lowering energy of 9.1 kcal/mol with the presence of oxidative $PhI(OAc)_2$. In **INT-3**, two acetate groups of $PhI(OAc)_2$ are released and coordinate with Pd. After then, the N–H bond of the substrate is activated by another AcO^- with a barrier of 18.8 kcal/mol through transition state **TS-2**. In contrast, the acetoxylation transition states **TS-2'** was also carefully considered, the C–O formation from Pd(IV) intermediate **INT-3**. Accordingly, the C–O formation barrier is higher than that of **TS-2** by 6.3 kcal/mol. Therefore, not surprisingly, the acetoxylation product should be excluded. After octahedral intermediate **INT4**, a transition state (**TS-3**) of ring closure is located by overcoming the relatively lower barrier of 7.6 kcal/mol. Subsequently, the generation of final product via the formation of the C–N bond undergoes reductive elimination with releasing the larger binding energy of around 33.8 kcal/mol. Interestingly, after intermediate **INT-4**, a more reactive unsaturated pentacoordinated Pd(IV) intermediate **INT-5** is generated by lowering energy of 10.2 kcal/mol with the dissociation of one

HOAc from Pd centre. Therefore, not surprisingly, the generation of pentacoordinated Pd(IV) intermediate **INT-5** is thermodynamically favorable. After then, transition state **TS-4** of ring closure is successfully located by overcoming the relatively lower barrier of 7.1 kcal/mol than that (7.6 kcal/mol) of hexacoordinated transition state **TS-3**. Subsequently, the generation of final product via the formation of the C–N bond undergoes reductive elimination with releasing the larger binding energy of around 23.1 kcal/mol. Figure S1 also showed the similar results are also obtained with C_{ethyl}–H activation from **INT-2-a** to final product.

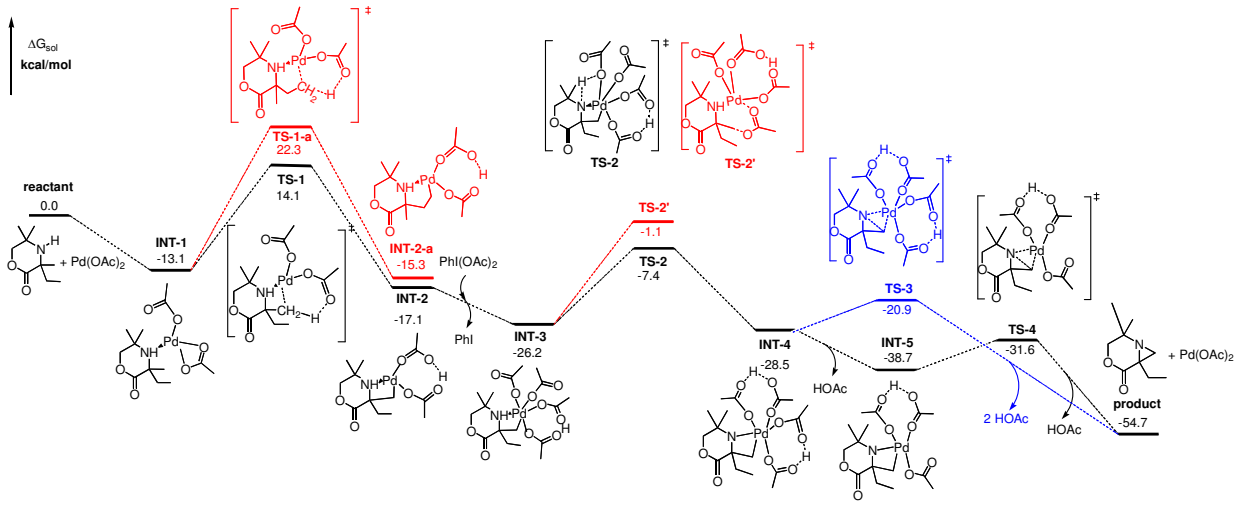

Figure 1 Potential Gibbs free energy (kcal/mol) profiles of the overall catalytic cycle. The most preferred pathway involving S configuration C_{methyl}–H activation is indicated by black colour.

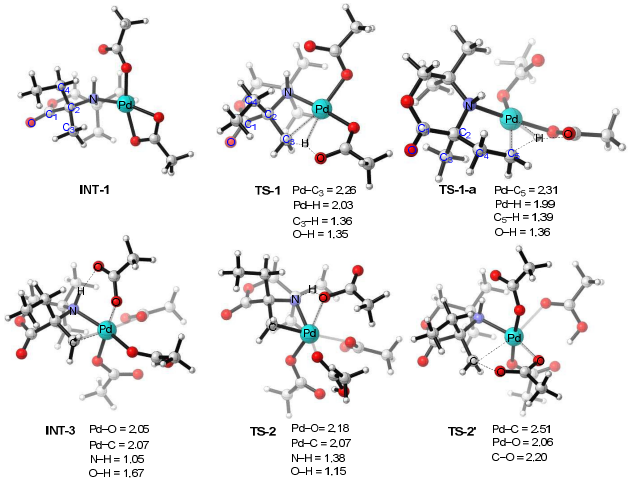

Figure 2 Optimized geometries of **INT-1**, the C–H activation transition states **TS-1** and **TS-1-a,** intermediate **INT-3**, the N–H activation transition state **TS-2**, and the acetoxylation transition state **TS-2'**. Selected distances are shown in Å.

As shown in Figure 2, the geometrical feature of **TS-1** is a four-centered interaction among the C_{methyl}–H, one O atom of AcO^- and Pd. The concomitant C–Pd bond elongate the C…H distance from 1.09 Å (**INT-1**) to 1.36 Å (**TS-1**). In the transition state **TS-1**, the C…Pd distance is 2.26 Å, and in **TS-1-a**, C…Pd distance is 2.31 Å, indicating a slight stronger Pd…C interaction in **TS-1**. Similarly, the length of C–H and C–O bond in **TS-1** (1.36 Å and 1.35 Å, respectively) are a little shorter than those in **TS-1-a** (1.39 Å and 1.36 Å, respectively). In methyl activation **TS-1**, the dihedral angle O–C_1–C_2–C_3 increases from 44.9˚ to 47.8˚. In contrast, in ethyl activation **TS-1-a**, the dihedral angle O–C_1–C_2–C_3 increases from –74.8˚ to –49.2˚ the dihedral angle changes is higher with 25.6˚. Therefore, it can be understood that ethyl activation is restricted by larger distortion than that of methyl activation for the C–H activation, suggesting a favorable C_{methyl}–H than C_{ethyl}–H activation. From **INT-3** to **TS-2**, the N…H distance is elongated from 1.05 Å (**INT-3**) to 1.38 Å (**TS-2**). Simultaneously, the Pd–O bond is elongated from 2.05 Å to 2.18 Å, the stronger O…H distance is shortened from 1.67 Å to 1.15 Å to promote N–H activation by AcO^-. In **TS-2'**, the Pd–C bond is elongated from 2.07 Å (**INT-3**) to 2.51 Å, one of the acetate is transferred to the methylene.

Terminal ethyl-C–H activation *vs* Methylene-C–H activation

Figure 3 shows the energy profile for the competed C–H activation of diethyl-substituted substrate: the five-membered palladacycle (Terminal ethyl-C–H activation) or the four-membered palladacycle (Methylene-C–H activation). In detail, transition state **B-TS-1** of the terminal ethyl C(sp^3)–H activation connects intermediate **B-INT-1** and five-membered palladacycle intermediate **B-INT-2** by overcoming a barrier of 21.6 kcal/mol. The Pd…C distance is shortened while the C–H bond is elongated from 1.09 Å (**B-INT-1**) to 1.39 Å (**B-TS-1**). In contrast, transition state **B-TS-1-a** of methylene-C(sp^3)–H activation connects intermediate **B-INT-1** and four-membered palladacycle intermediate **B-INT-2-a** with a relatively higher barrier of 29.0 kcal/mol, indicating a more favorable terminal C–H activation than methylene C–H activation. In **B-TS-1-a**, the

Pd…C distance (2.30 Å) is a little longer than that (2.24 Å) in **B-TS-1**, and the C–H bond is elongated from 1.09 Å (**B-INT-1**) to 1.44 Å (**B-TS-1-a**).

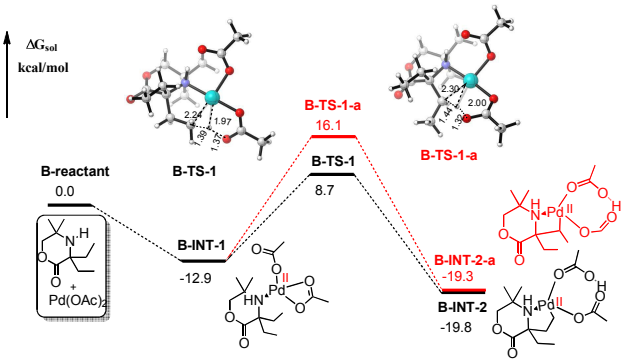

Figure 3 Potential free energy profile for C–H activations of diethyl-substituted substrate. Gibbs free energies are given in kcal/mol. Selected distances are shown in Å.

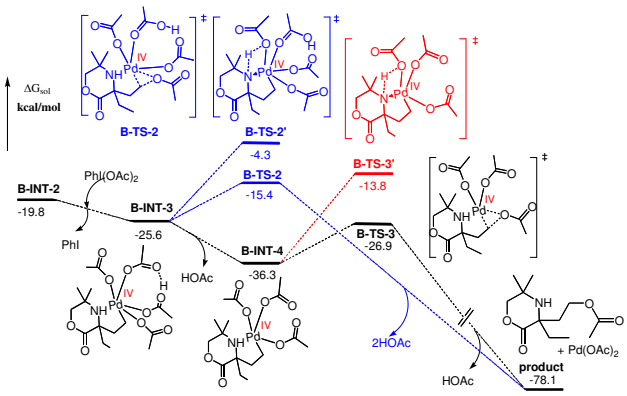

Figure 4 Potential free energy profile for the catalytic cycle. Gibbs free energies are given in kcal/mol.

In the following step, an octahedral Pd(IV) intermediate **B-INT-3** will be generated by the presence of oxidative PhI(OAc)$_2$, which is more stable than **B-INT-2** by 5.8 kcal/mol, as shown in Figure 4. Starting from **B-INT-3**, it may potentially undergo transition state **B-TS-2** by C–O formation with a relatively lower barrier of 10.2 kcal/mol. Subsequently, **B-TS-2** undergoes reductive elimination to give the final acetoxylation product by releasing the larger amount of energy of 62.7 kcal/mol. Interestingly, during our calculations, the N–H activation (transition state **B-TS-2'**) may occur by connecting **B-INT-3** and final product with a relatively larger barrier of 21.3 kcal/mol than that of the corresponding C–O interaction (10.2 kcal/mol) in **B-TS-2**, leading to the aziridine product after reductive elimination. Also as previously discussed, a more thermodynamically stable pentacoordinated Pd(IV) intermediate **B-INT-4** is formed by one HOAc dissociation, releasing 10.7 kcal/mol of free energy from **B-INT-3**. After **B-INT-4**, it may potentially undergo transition state **B-TS-3** by C–O formation with a relatively lower barrier of 9.4 kcal/mol. Subsequently, **B-TS-3** undergoes reductive elimination to give the final acetoxylation product by releasing the larger amount of energy of 51.2 kcal/mol. Interestingly, during our calculations, the N–H activation (transition state **B-TS-3'**) may also occur by connecting **B-INT-4** and final product with a relatively larger barrier of 22.5 kcal/mol than that of the corresponding C–O interaction (9.4 kcal/mol) in **B-TS-3**, leading to the aziridine product after reductive elimination. Based on these data, the pathway through hexacoordinated intermediate **B-INT-3** is unlikely because of its high activation energy. Therefore, not surprisingly, the C–O formation is more favorable from **B-INT-4** to final acetoxylation product than aziridine product. It is in good agreement with the experiment results.[13]

Aziridine *vs* acetoxylation product from the absence of lactone. Figure 5 shows the energy profile for the competing C–H activation of dimethyl-substituted substrate. In detail, the reaction is initiated with aliphatic amines and Pd(OAc)$_2$. After coordination, intermediate **C-INT-1**, a tetra-coordinated Pd(II) intermediate is located by 14.1 kcal/mol more stable than reactants. After **C-INT-1**, a C(sp^3)–H cleavage via the acetate-enabled concerted metalation-deprotonation (CMD) mechanism is favored. Figure 5 shows the rate-determining transition state **C-TS-1** connects intermediate **C-INT-1** and **C-INT-2** with a relatively higher barrier of 26.5 kcal/mol. Similarly, a more stable six-coordinated Pd(IV) intermediate **C-INT-3** is formed after the oxidation of the PhI(OAc)$_2$, releasing energy of 11.4 kcal/mol. In the following step, the C–O coupling takes place through transition state **C-TS-2**, which shows the migration of OAc$^-$ anion to C atom of methylene with a relatively lower barrier of 13.3 kcal/mol, leading to final acetoxylation product by releasing the larger amount of energy of 66.1 kcal/mol. In contrast, the N–H activation transition state **C-TS-2-a** connects intermediate **C-INT-3** and **C-INT-4-a** with a relatively larger barrier of 20.1 kcal/mol than that of the corresponding C–O coupling. After **C-INT-4-a**, the reductive elimination from Pd(IV) to Pd (II) step is located through **C-TS-4-a** with a relatively lower barrier of 6.2 kcal/mol than that of the N–H activation. A three-membered ring is then formed in aziridine product, releasing a large amount of energy of 51.2 kcal/mol. And the dissociation of the acetate of the Pd center is an exothermic process. Admittedly, as shown in Figure 5, the dissociation of one HOAc takes place exothermically via **C-INT-3** by releasing 6.3 kcal/mol of free energy to form a more thermodynamically stable pentacoordinated Pd(IV) intermediate **C-INT-4**. A subsequent reductive elimination reaction leads to final acetoxylation product via transition state **C-TS-3** with a barrier of 14.4 kcal/mol. Transition state **C-TS-3** would lead to the irreversible formation of acetoxylation product in an exothermic reaction that releases 60.9 kcal/mol of free energy. Also, the N–H activation pentacoordinated transition state **C-TS-3-a** connects intermediate **C-INT-4** and **C-INT-5-a** with a relatively larger barrier of 22.1 kcal/mol than

Journal Name

ARTICLE

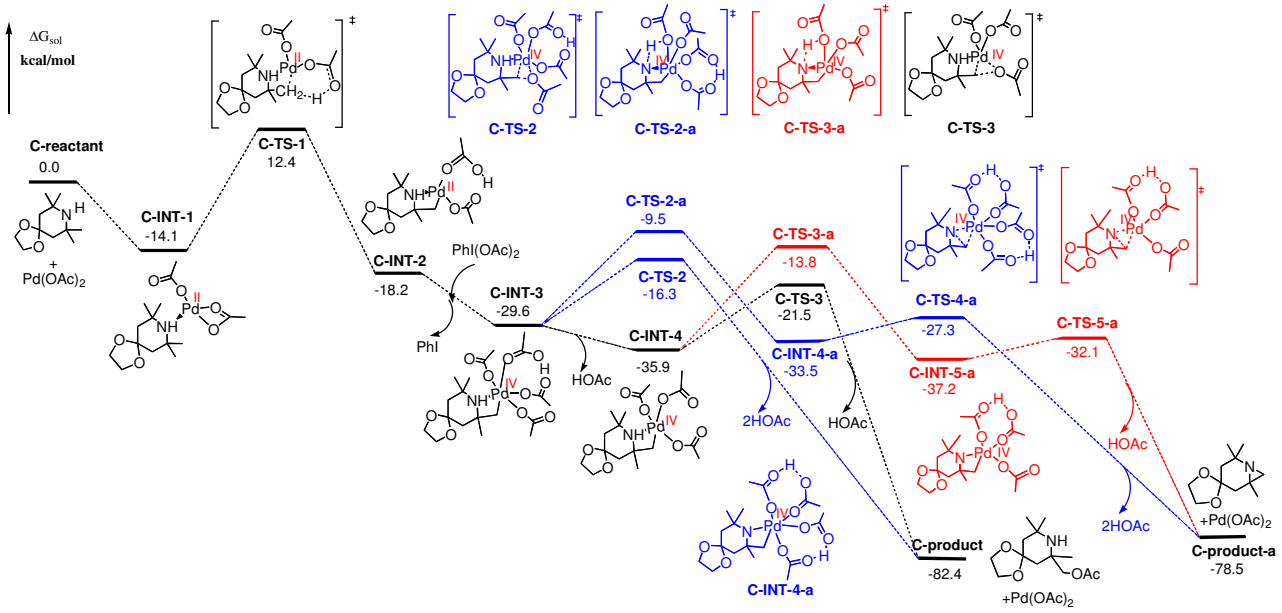

Figure 5 Potential Gibbs free energy (kcal/mol) profile for the competing C–H activation of dimethyl-substituted none lactone substrate.

that of the corresponding C–O coupling transition state **C-TS-3**. After **C-INT-5-a**, a three-membered ring is then formed via transition state **C-TS-5-a** with a relatively lower barrier of 5.1 kcal/mol. The overall process from **C-INT-5-a** to aziridine product is also exothermic and irreversible and releases 46.4 kcal/mol of free energy. Based on the discussions above, it is clear that the pentacoordinated Pd(IV) intermediate **C-INT-4** is most favorable because of its thermodynamical stability. Notable is the difference between the barrier of formation of acetoxylation and aziridine product, indicating that the acetoxylation product process is kinetically and thermodynamically favorable than aziridine product process, which is in good agreement with the experimental observations.

Conclusions

In summary, the mechanism of palladium-catalyzed aliphatic amine C(sp^3)–H activation has been performed using density functional theory computational methods. The catalyst-substrate complex consisting of coordination through a nitrogen is favorable for ensuing C–H activation. Selectivity issues in the C–H activation step have been analyzed, the C_{methyl}–H bond activation takes place through unexpected four-membered transition state. DFT calculations showed that C–H activation is the rate-determining step and the acetate assisted CMD mode happened in this deprotonation step. Theoretical calculations also indicated that pentacoordinated Pd(IV) intermediates are thermodynamically and kinetically more favorable than the corresponding hexacoordinated intermediates. When the diethyl-substituted exist in the morpholine structure, the terminal ethyl C(sp^3)–H bond is more reactivated than the C–H bond of methylene, and prefers to form the acetoxylation product. In the absence of the lactone substrate, the directing acetoxylation product is kinetically and thermodynamically favorable, which is in good agreement with Gaunt's observations. The results may enrich the understanding of Pd-catalyzed C–H activation on cyclic aliphatic amines and could serve as a benchmark for regioselectivity. We hope these theoretical insights could serve as stimulation and guideline for experimental efforts in this field.

Acknowledgements

The authors thank the reviewer for the constructive and pertinent comments. The authors appreciate the financial support from Starting-up Foundation (Q410900111 and Q410900211) and Scientific Research Foundation of Soochow University

(SDY2012A07), and Natural Science Foundation of China (21201127). This project was funded by the Priority Academic Program Development of Jiangsu Higher Education Institutions (PAPD).

Notes and references

1 (a) C. Jia, T. Kitamura, Y. Fujiwara, *Acc. Chem. Res*., 2001, **34**, 633; (b) F. Kakiuchi, N. Chatani, *Adv. Synth. Catal*., 2003, **345**, 1077; (c) K. Godula, D. Sames, *Science*, 2006, **312**, 67; (d) A. R. Dick, M. S. Sanford, *Tetrahedron*, 2006, **62**, 2439; (e) H. M. L. Davies, J. R. Manning, *Nature*, 2008, **451**, 417; (f) R. Giri, B.-F. Shi, K. M. Engle, N. Maugel, J.-Q. Yu, *Chem. Soc. Rev*., 2009, **38**, 3242; (g) I. A. I. Mkhalid, J. H. Barnard, T. B. Marder, J. M. Murphy, J. F. Hartwig, *Chem. Rev*., 2010, **110**, 890; (h) H. M. L. Davies, Bois, J. Du, J.-Q. Yu, *Chem. Soc. Rev*., 2011, **40**, 1855; (i) N. Kuhl, M. N. Hopkinson, J. Wencel-Delord, F. Glorius, *Angew. Chem., Int. Ed*., 2012, **51**, 10236.

2 (a) T. W. Lyons, M. S. Sanford, *Chem. Rev*., 2010, **110**, 1147; (b) D. Alberico, M. E. Scott, M. Lautens, *Chem. Rev*., 2007, **107**, 174.

3 (a) I. V. Seregin, V. Gevorgyan, *Chem. Soc. Rev*., 2007, **36**, 1173; (b) O. Daugulis, H.-Q. Do, D. Shabashov, *Acc. Chem. Res.* 2009, **42**, 1074; (c) K. M. Engle, T.-S. Mei, M. Wasa, J.-Q. Yu, *Acc. Chem. Res*., 2012, **45**, 788; (d) S. R. Neufeldt, M. S. Sanford, *Acc. Chem. Res*., 2012, **45**, 936; (e) R. Tang, G. Li, J.-Q. Yu, *Nature*, 2014, **507**, 215; (f) Y.-J. Liu, H. Xu, W.-J. Kong, M. Shang, H.-X. Dai, J.-Q. Yu, *Nature*, 2014, **515**, 389.

4 (a) L. V. Desai, K. L. Hull, M. S. Sanford, *J. Am. Chem. Soc*., 2004, **126**, 9542; (b) A. R. Dick, J. W. Kampf, M. S. Sanford, *J. Am. Chem. Soc.* 2005, **127**, 12790; (c) D. Balcells, E. Clot, O. Eisenstein, *Chem. Rev*., 2010, **110**, 749; (d) A. J. Hickman, M. S. Sanford, *Nature,* 2012, **484**, 177; (e) M. D. Lotz, M. S. Remy, D. B. Lao, A. Ariafard, B. F. Yates, A. J. Canty, J. M. Mayer, M. S. Sanford, *J. Am. Chem. Soc*., 2014, **13**6, 8237; (f) W. Du, Q.-S. Gu, Z.-L. Li, D. Yang, *J. Am. Chem. Soc*., 2015, **137**, 1130; (g) K. S. L. Chan, H.-Y. Fu, J.-Q Yu, *J. Am. Chem. Soc*., 2015, **137**, 2042.

5 (a) P. W. N. M. van Leeuwen, *Homogeneous Catalysis: Understanding the Art,* Kluwer Academic Publishers, Dordrecht, 2004; (b) L. F. Tietze, G. Brasche, K. M. Gericke, *Domino Reactions in Organic Synthesis;* Wiley-VCH: Weinheim, 2006; (c) J. F. Hartwig, *Organotransition Metal Chemistry: From Bonding to Catalysis,* University Science Books, Sausalito, 2010; (d) R. F. Heck, *Acc. Chem. Res.*, 1979, **12**, 146; (e) A. Suzuki, *Chem. Commun.* 2005, 4759; (f) M. Aufiero, F. Proutiere, F. Schoenebeck, *Angew. Chem., Int. Ed.*, 2012, **51**, 7226; (g) Z.-H. He, S. Kirchberg, R. Frohlich, A. Studer, *Angew. Chem., Int. Ed.,* 2012, **51**, 3699.

6 (a) L. M. Mirica, J. R. Khusnutdinova, *Coord. Chem. Rev.*, 2013, **257**, 299; (b) R. van Belzen, H. Hoffmann, C. J. Elsevier, *Angew. Chem., Int. Ed.*, 1997, **36**, 1743; (c) Y. Yamamoto, T. Ohno, K. Itoh, *Angew. Chem., Int. Ed*., 2002, **41**, 3662. (d) S. R.Whitfield, M. S. Sanford, *J. Am. Chem. Soc.,* 2007, **129**, 15142; (e) T. Furuya, T. Ritter, *J. Am. Chem. Soc.,* 2008, **130**, 10060; (f) D. C. Powers, T. Ritter, *Nat. Chem.*, 2009, **1**, 302; (g) T. Furuya, D. Benitez, E. Tkatchouk, A. E. Strom, P. Tang, W. A. Goddard , T. Ritter, *J. Am. Chem. Soc.*, 2010, **132**, 3793; (h) Y.-F. Dang, S.-L. Qu, J. W. Nelson, H. D. Pham, Z.-X. Wang, X.-T, Wang, *J. Am. Chem. Soc.,* 2015, **137**, 2006. (i) B. E. Haines, H. Y. Xu, P. Verma, X.-C. Wang, J.-Q. Yu, D. G. Musaev, *J. Am. Chem. Soc.*, 2015, **137**, 9022.

7 (a) D. C. Powers, T. Ritter, *Acc. Chem. Res*., 2012, **45**, 840; (b) D. C. Powers, D. Benitez, E. Tkatchouk, W. A. Goddard, T. Ritter, *J. Am. Chem. Soc*., 2010, **132**, 14092 ;(c) D.C. Powers, T. Ritter, *Top. Organomet. Chem.*, 2011, **35**, 129; (d) D. C. Powers, D. Y. Xiao, M. A. L. Geibel, T. Ritter, *J. Am. Chem. Soc*., 2010, **132**, 14530.

8 (a) D. C. Powers, E. Lee, A. Ariafard, M. S. Sanford, B. F. Yates, A. J. Canty, T. Ritter, *J. Am. Chem. Soc*., 2012, **134**, 12002. (b) G. Maestri, E. Motti, N. D. Ca', M. Malacria, E. Derat, M. Catellani, *J. Am. Chem. Soc*., 2011, **133**, 8574; (c) G. Maestri, M. Malacria, E. Derat, *Chem. Commun.*, 2013, **49**, 10424; (d) D. C. Powers, T. Ritter, *Organometallics*, 2013, **32**, 2042; (e) F.-Z .Tang, F.-R. Qu, J. R. Khusnutdinova, N. P. Rathb, L. M. Mirica, *Dalton Trans*., 2012, **41**, 14046; (f) A. J. Canty, A. Ariafard, M. S. Sanford, B. F. Yates, *Organometallics*, 2013, **32**, 544.

9 (a) Q.-W. Yao, E. P. Kinney, Z. Yang, *J. Org. Chem*., 2003, **68**, 7528; (b) Atsushi. Ishikawa, Yoshihide. Nakao, Hirofumi. Satoa, Shigeyoshi. Sakaki, *Dalton Trans*., 2010, **39**, 3279; (c) Y. Wei, W.-P. Su, *J. Am. Chem. Soc*., 2010, **132**, 16377; (d) K. Kawasumi, K. Mochida, T. Kajino, Y Segawa, K. Itami, *Org. Lett*., 2012, **14**, 418.

10 (a) N. R. Deprez, D. Kalyani, A. Krause, M. S. Sanford, *J. Am. Chem. Soc*., 2006, **128**, 4972; (b) E. A. Merritt, B. Olofsson, *Angew. Chem., Int. Ed.,* 2009*,* **48***,* 9052.

11 (a) V. G. Zaitsev, D. Shabashov, O. Daugulis, *J. Am. Chem. Soc*., 2005, **127**, 13154; (b) D. Shabashov, O. Daugulis, *J. Am. Chem. Soc*., 2010, **132**, 3965; (c) L. Ackermann, *Chem. Rev*., 2011, **111**, 1315; (d) L. Dieu Tran, O Daugulis, *Angew. Chem., Int. Ed.,* 2012, **51**, 5188; (e) J. He, S.-H. Li, Y.-Q. Deng, H.-Y. Fu, B. N. Laforteza, J. E. Spangler, A. Homs, J.-Q. Yu, *Science*, 2014, **343**, 1216.

12 (a) R. J. Phipps, M. J. Gaunt, *Science*, 2009, **323**, 1593; (b) J. F. Hartwig, *Chem. Soc. Rev*., 2011, **40**, 1992; (c) M. J. Tredwell, M. Gulias, N. G. Bremeyer, C. C. C. Johansson, B. S. L. Collins, M. J. Gaunt, *Angew. Chem., Int. Ed*., 2011, **50**, 1076; (d) D. S. Leow, Li. Gang, T.-S. Mei, J.-Q. Yu, *Nature*, 2012, **486**, 518; (e) M. Bera, A. Modak, T. Patra, A. Maji, D. Maiti, *Org. Lett*., 2014, **16**, 5760; (f) Y. Nakanoa, D. W. Lupton, *Chem. Commun*., 2014, **50**, 1757.

13 V. G. Zaitsev, D. Shibashov, O. Daugulis, *J. Am. Chem. Soc*., 2005, **127**, 13154.

14 B. V. Subba Reddy, L. Rajender Reddy, E. J. Corey, *Org. Lett*., 2006, **8**, 3391.

15 D. A. Colby, R. G. Bergman, J. A. Ellman, *Chem. Rev*., 2010, **110**, 624.

16 (a) D. García-Cuadrado, A. A. C. Braga, F. Maseras, A. M. Echavarren, J*. Am. Chem. Soc*., 2006, **128**, 1066; (b) M. Lafrance, S. I. Gorelsky, K. Fagnou, *J. Am. Chem. Soc*., 2007, **129**, 14570. (c) S. I. Gorelsky, D. Lapointe, K. Fagnou, *J. Am. Chem. Soc.*, 2008, **130**, 10848; (d) S. Rousseaux, M. Davi, J. Sofack-Kreutzer, C. Pierre, C. E. Kefalidis, E. Clot, K. Fagnou, *J. Am. Chem. Soc*., 2010, **132**, 10706; (e) D. Balcells, E. Clot, O.Eisenstein, *Chem. Rev*., 2010, **110**, 749; (f) I. A. Sanhueza, A. M. Wagner, M. S. Sanford, F. Schoenebeck, *Chem. Sci*., 2013, **4**, 2767; (g) Y.-F. Yang, G.-J. Cheng, P. Liu, D. Leow, T.-Y. Sun, P. Chen, X. Zhang, J.-Q. Yu, Y.-D. Wu, K. N. Houk, *J. Am. Chem. Soc.,* 2014, **136**, 344.

17 A. McNally, B. Haffemayer, B. S. L. Collons, M. J. Gaunt, *Nature*, 2014, **510**, 129.

18 A. D. Becke, *J. Chem. Phys*., 1993, **98**, 5648.

19 M. J. Frisch, G. W. Trucks, H. B. Schlegel, G. E. Scuseria, M. A. Robb, J. R. Cheeseman, G. Scalmani, V. Barone, B. Mennucci, G. A. Petersson, G. H. Nakatsuji, M. Caricato, X. Li, H. P. Hratchian, A. F. Izmaylov, J. Bloino, G. Zheng, J. L. Sonnenberg, M. Hada, M. Ehara, K. Toyota, R. Fukuda, J. Hasegawa, M. Ishida, T. Nakajima, Y. Honda, O. Kitao, H. Nakai, T. Vreven, Jr. J. A. Montgomery, J. E. Peralta, F. Ogliaro, M. Bearpark, J. J. Heyd, E. Brothers, K. N. Kudin, V. N. Staroverov, R. Kobayashi, J. Normand, K. Raghavachari, A. Rendell, J. C. Burant, S. S. Iyengar, J. Tomasi, M. Cossi, N. Rega, J. M. Millam, M. Klene, J. E. Knox, J. B. Cross, V.

Bakken, C. Adamo, J. Jaramillo, R. Gomperts, R. E. Stratmann, O. Yazyev, A. J. Austin, R. Cammi, C. Pomelli, J. W. Ochterski, R. L. Martin, K. Morokuma, V. G. Zakrzewski, G. A. Voth, P. Salvador, J. J. Dannenberg, S. Dapprich, A. D. Daniels, Ö. Farkas, J. B. Foresman, J. V. Ortiz, J. Cioslowski and D. J. Fox, *Gaussian, 09, Revision C.01*, Gaussian, Inc., Wallingford CT, 2010.

20 (a) P. J. Hay, W. R. J. Wadt, *Chem. Phys*., 1985, **82**, 270; (b) W. R. Wadt, P. J. J. Hay, *Chem. Phys*., 1985, **82**, 284.

21 P. C. Hariharan, J. A. Pople, *Theor. Chim. Acta.,* 1973, **28**, 213.

22 (a) K. J. Fukui, *Phys. Chem*., 1970, **74**, 4161; (b) K. Fukui, *Acc. Chem. Res*., 1981, **14**, 363.

23 A. V. Marenich, C. J. Cramer, D. G. Truhlar, *J. Phys. Chem. B*., 2009, **113**, 6378.

24 C. Y. Legault, CYLview, 1.0 b, Université de Sherbrooke, Quebec(Canada), 2009, (http ://www.cylview.org).

25 (a) Y. Tan, J. F. Hartwig, *J. Am. Chem. Soc*., 2011, **133**, 3308. (b) A. K. Cook, M. S. Sanford, *J. Am. Chem. Soc*., 2015, **137**, 3109.